Refractivity compensated tracking interferometer for precision engineering

Karl Meiners-Hagen[1], Florian Pollinger[1], Günther Prellinger[1], Kerstin Rost[1], Klaus Wendt[1], Wolfgang Pöschel[2], Denis Dontsov[2], Walter Schott[2], Viktor Mandryka[2]

[1]Physikalisch-Technische Bundesanstalt, Bundesallee 100, D-38116 Braunschweig
[2]SIOS Meßtechnik GmbH, Am Vogelherd 46, D-98693 Ilmenau

ABSTRACT

Coordinate measurements are a standard task in industry. For larger volumes tracking devices are used, which optically measure 3D coordinates by different techniques, e.g. by interferometry or time of flight measurement. For these the refractive index plays an important role for the achievable measurement uncertainty. Within a European joint research program, PTB and SIOS develop a tracking device with internal compensation of the refractive index by using two different wavelengths. In a first step a prototype interferometer was set up for testing the components. First 1D results up to a length of six meters are presented. The prototype turned out to be mechanically not stable enough, but the compensation of the refractive index could be demonstrated clearly. Since this refractive index compensation method increases the uncertainty by a quite large constant factor, a procedure for averaging via optically measured temperatures while retaining the time resolution of the position data was developed.

Index Terms - Interferometry, refractive index compensation, laser tracker

1. INTRODUCTION

As part of a European joint research program (JRP), PTB and SIOS develop a tracking interferometer. In the JRP IND53 “Large Volume Metrology in Industry” several new measuring tools and techniques based on several different operating principles are developed that are capable of operation in typical industrial environments. These include new traceable absolute distance meters with operation ranges of at least 20 meters, line-of-sight refractive index measuring systems, and novel multi-sensor systems that can measure refractive index effects in a 3D volume. These systems will enable on-line compensation of refractive index effects in industrial environments in volumes of up to of 10 m × 10 m × 5 m with a target accuracy of 1 part in 10^7.
The interferometer head is designed for tracking the retroreflector. The returning measurement beam from the reflector is focused onto a steel sphere and interferes with the reference beam after the reflection at the sphere. In this configuration essentially the distance between the fixed sphere and the moving retroreflector is measured and uncertainties due to the movement of the interferometer are greatly reduced. The basic design is similar to the “LaserTRACER” of the company Etalon [1].
Optical length measurements in industrial environments suffer from the imperfect knowledge of the refractive index of air, especially the precise measurement of air temperature is difficult when gradients and turbulences are present. By measuring a length using an interferometer with two different wavelengths simultaneously, the dispersion of air can be used to compensate for the influence of the refractive index. This technique is known since the late 1960s [2] but the basic method is valid only for dry air. In presence of air humidity it is possible to determine the partial pressure of water vapor and compensate the refractive index with a modified equation [3].

We implemented this technique by using a frequency doubled Nd:YAG laser as the light source for the interferometer. For testing and optimization of the system an interferometer head build from standard optomechanical components without tracking capability was developed. First results and the detailed procedure of applying the refractive index compensation are presented in the following sections.

2. THEORY OF REFRACTIVE INDEX COMPENSATION

An interferometer measures the optical path difference *nl* between its both arms. To get the actual length *l*, the refractive index of air *n* has to be known, which depends on the air temperature *t*, pressure *p*, relative humidity *RH* respective the partial pressure of water vapor p_w, and to a minor degree on the composition of the air (mainly CO_2 content *x*). The refractive index is then calculated from these parameters using empirical formulas (e.g. [4], [5]). Especially the precise measurement of the air temperature in the beam path is difficult due to relatively slow sensors and temperature gradients. An uncertainty of one Kelvin leads to nearly 10^{-6} in length.
Since the 1960s a compensation method for the refractive index is known by measuring the length with two wavelengths $\lambda_{1,2}$ simultaneously [2]. Such a measurement results in two different optical path differences $n_{1,2}l_{1,2}$ due to the dispersion in air. With an equation for the refractive index the length *l* can be calculated. Within this paper the equation of Bönsch and Potulski is used [5]. The structure of the equation is

$$n(\lambda, t, p, x, p_w) - 1 = K(\lambda) \cdot D(t, p, x) - p_w \cdot g(\lambda) \tag{1}$$

with

$$K(\lambda) = 10^{-8}\left(8091.37 + \frac{2333983}{130 - 1/(\lambda/\mu\mathrm{m})^2} + \frac{15518}{38.9 - 1/(\lambda/\mu\mathrm{m})^2}\right), \tag{2}$$

$$g(\lambda) = 10^{-10}(3.802 - 0.0384/(\lambda^2/\mu\mathrm{m})^2), \tag{3}$$

and

$$D(t, p, x) = \frac{p/\mathrm{Pa}}{932164.60} \frac{1 + 10^{-8}(0.5953 - 0.009876\, t/^{\circ}\mathrm{C})\, p/\mathrm{Pa}}{1 + 0.0036610\, t/^{\circ}\mathrm{C}} \times (1 + 0.5327(x - 0.0004)). \tag{4}$$

In dry air ($p_w = 0$) the length is given by:

$$l = l_1 - A(l_2 - l_1) \tag{5}$$

with

$$A = \frac{n_1 - 1}{n_2 - n_1}.$$

In the factor *A* the function *D*(*t*,*p*,*x*) cancels out and the factor depends only on the wavelengths. Therefore, the length can be measured without knowledge of the air parameters. However, the factor is quite large, e.g. $A \approx 65.5$ for the wavelength pair 1064 nm and 532 nm used in our set-up. Measurement uncertainties for both optical path differences are scaled up by this factor. For moist air the air parameters do not cancel out and *A* depends on all air parameters.

However, a solution can be found including water vapor [3]. The length is then given by the equation:

$$l = \frac{K(\lambda_1)l_2 - K(\lambda_2)l_1}{K(\lambda_1) - K(\lambda_2) + (p_w/\mathrm{Pa})(g(\lambda_1)K(\lambda_2) - g(\lambda_2)K(\lambda_1))}. \quad (6)$$

Only the partial pressure of water vapor remains in the calculation of the length and has to be measured separately. This can be done by measuring the relative humidity with a standard hygrometer and calculate p_w with the ambient temperature of the sensor. Although there is no explicit factor A in equation 6, the scaling of the uncertainties in the length difference by almost the same amount is also present.

In addition to the length the effective air temperature in the beam path can also be derived from the optical path difference if the air pressure is known. Please note that in reference [3] the equation for the temperature has an error. In the term $(l_2 - l_1)\delta$ in the denominator the lengths are exchanged. The correct equation for the temperature is:

$$t = \frac{\alpha(p + \beta p^2)L_k - p_w L_g + l_2 - l_1}{\alpha\gamma p^2 L_k + p_w L_g \delta + (l_1 - l_2)\delta} \quad (7)$$

with

$$L_k = l_2 K(\lambda_1) - l_1 K(\lambda_2)$$
$$L_g = l_2 g(\lambda_1) - l_1 g(\lambda_2)$$

and

$$\alpha = \frac{1 + 0.5327(x/\mathrm{ppm} - 400) \times 10^{-6}}{93214.6}$$
$$\beta = 0.5953 \times 10^{-8}$$
$$\gamma = 0.009876 \times 10^{-8}$$
$$\delta = 0.003661$$

The thus derived temperature is not necessary for the direct determination of the length but it can be helpful for averaging the results to reduce the uncertainties introduced by the large factor A. This will be presented in detail in section 4.

3. EXPERIMENTAL SET-UP

A frequency doubled Nd:YAG laser (Innolight Prometheus 20) with wavelengths of 1064 nm and 532 nm serves as the light source. For interferometric length measurements the laser frequency must be stabilized. A Doppler free hyperfine absorption line of iodine at 532 nm wavelength is used for this. The iodine stabilization of the laser is a standard 3f stabilization except for the modulation of the laser frequency. Usually the pump current of the laser is modulated. This would result in a modulation of the length measurement of the interferometer. Therefore, the modulation is done by frequency modulation of an acousto-optic modulator (AOM) with a rate of 2.7 kHz (figure 1). With a double pass through the frequency shifter the variation of the deflection angle with frequency is almost eliminated.

The photo diode (PD) signal is fed into a lock-in amplifier (Stanford SR850) in 3f mode. The output is connected to a PI controller which controls the voltage of the internal piezo crystal in the laser.

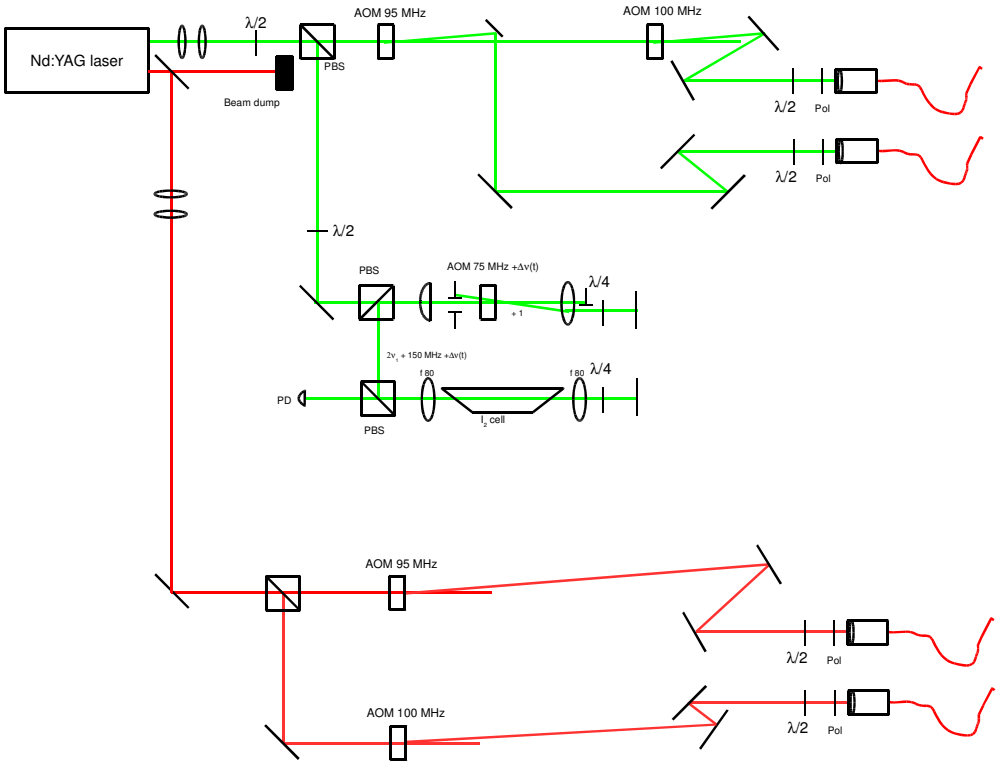

Figure 1: Optical set-up of the beam generation.

For the operation of the interferometer a heterodyne technique is used. For that purpose the laser beams of both wavelengths are split in two parts which are frequency shifted by different amounts (100 MHz and 95 MHz) with four AOMs. The four resulting beams are coupled into polarization maintaining singe mode fibers. A λ/2 wave plate and a polarizer in front of each fiber collimator align the polarization to the fiber axes.

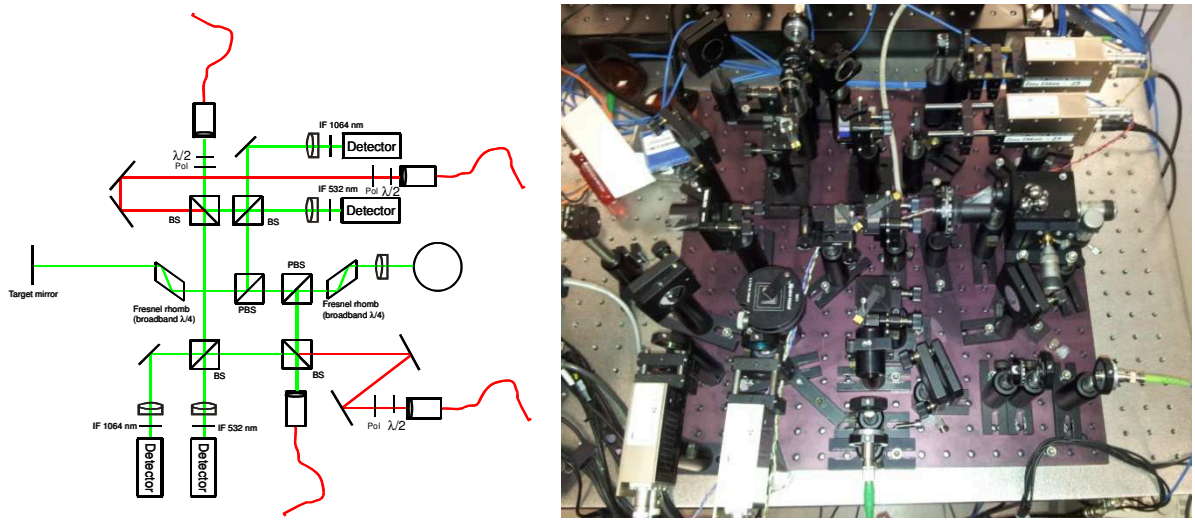

Figure 2: Schematics and photo of the prototype interferometer head.

For first tests and optimizations a prototype interferometer head was set up from standard optomechanical components. The optical set-up of the interferometer head is depicted in figure 2. At each fiber output a λ/2 wave plate and a polarizer aligns the polarization to the s-polarization of the polarizing beam splitters (PBS). The 532 nm measurement beam emerging from the lower fiber is reflected by the PBS to the right. A Fresnel rhomb in this beam path acts as a broadband λ/4 waveplate (from 400 nm to 2000 nm). The beam is then focused by an achromatic lens onto the surface of a 12 mm steel sphere. For the final set-up a ~25 mm sphere will be used but was not available with a high quality surface. The sphere is positioned on top of three identical spheres which are glued together and mounted on a precision xyz-stage. With this mounting the sphere can be rotated in place to simulate the rotation of the final measuring head. In the final design the measurement beam is firstly directed onto the reflector and then to the sphere.
The beam which is reflected from the sphere is then recollimated by the lens and passed through both PBS. A second Fresnel rhomb switches the linear polarization into a circular one again and directs the beam onto the target reflector, which was a plane mirror for the first tests and alignment. The reflected beam leaves the left PBS to the top and is combined with the "local oscillator" beam from the upper fiber by a non polarizing beamsplitter (BS). The beam is finally focused through an interference filter for 532 nm on a photo detector (Femto HCA-S-200M-SI), where a 5 MHz signal with a phase proportional to the length appears.
A second path combines both beams on the breadboard to get a reference signal for the interferometer. The phase of the reference signal is subtracted from the phase of the measurement signal to eliminate phase changes from vibration or drift due to the optical fibers and the frequency shifters (AOMs).
The 1064 nm beams are aligned on the same paths as the 532 nm beams by two mirrors each. Two additional photo detectors (Femto HCA-S-200M-IN) equipped with interference filters for 1064 nm in front of them detect the corresponding signals.
From this prototype SIOS constructed a miniaturized version for mounting on a modified laser tracer base. Since the Fresnel rhombs are too bulky, λ/4 waveplates for 532 nm and 1064 nm simultaneously were used. The device is completed but was unfortunately not yet fully operational to make measurements for this paper.

The processing of the interferometer signals is done with an A/D converter with eight channels with 16 bit at 100 MSamples/s and a FPGA with 32 MB memory for each two channels (Model, SIS3302, Struck Innovative Systeme, Germany). A VHDL program was developed which detects the signal phase at the heterodyne frequency (5 MHz) in each channel [6].
For the phase calculation a block of 1200 raw samples (12 µs) is multiplied with two reference sine and cosine signals and the results are totalised. The reference signals are a 5 MHz sine and cosine with a Gaussian amplitude shape. They are precalculated and stored in tables. The sums are proportional to the sine and cosine of the corresponding signal phase $\Phi_{1,2}$. From these values the sine and cosine of the phase difference of two channels is calculated. A personal computer reads the data via USB. The data format is $a \sin(\Phi_2-\Phi_1)$, $a \cos(\Phi_2-\Phi_1)$. The advantage of this method is a reduction of the data rate by a factor of two. The disadvantage is that the amplitude a of both channels cannot be measured separately. However, the reference signal from the interferometer is stable and decreasing amplitude indicates a loss of the measurement signal.

4. EXPERIMENTAL RESULTS

The prototype interferometer head with standard optomechanical components turned out to be far less stable than expected. For a measurement of the short term stability the interferometer was placed on an optical table with air damping. A plane mirror was mounted directly in front of the Fresnel rhomb as the reflector for the measurement beam. During the measurements a set of 8192 phase values with an averaging time of 12 µs are sampled by the AD-converter and saved in a file. The data for 8192 samples (98.3 ms) are shown in Figure 3. There are fast vibrations with approximately 2 nm amplitude and the difference between the 532 nm and 1064 nm length results varies by 0.5 nm. The 2 nm vibrations are a quite good result for this set-up but the 0.5 nm change in the length difference would indicate a length change of $0.5\ \text{nm} \times 65.5 = 33\ \text{nm}$ for the refractive index compensated result which is not reasonable. As the beam paths for 532 nm and 1064 nm wavelengths share most of the optical components, the mirrors and beamsplitters for directing the infrared beams on the path of the greens beam are the most probable source for this difference.

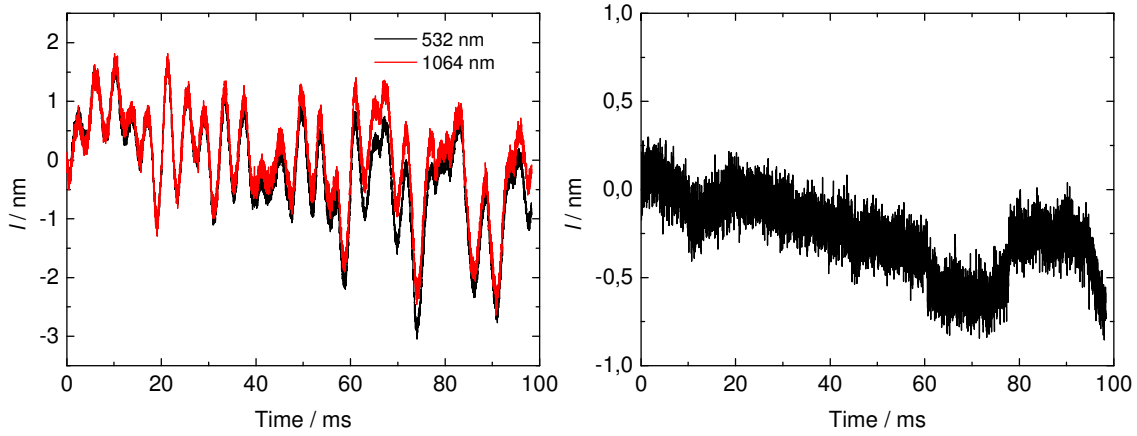

Figure 3: Short term stability of the interferometer. In the left figure the length results for 532 nm and 1064 nm are shown and in the right figure the difference between them.

For a further analysis of the stability the interferometer was aligned together with a HeNe reference interferometer along a 25 cm long rail with the beam path of both interferometers folded by a large triple mirror, giving a measuring range of 50 cm. A small triple mirror was used as reflector for the interferometer. In figure 4 the recorded length changes within 18 minutes at a fixed reflector position are depicted. The refractive index was calculated with the Edlen equation. While the HeNe interferometer drifts by approximately 90 nm the prototype interferometer drifts almost 500 nm in the opposite direction. The difference between 532 nm and 1064 nm result has no systematic variation but a standard deviation of 1.2 nm. This leads to $1.2\ \text{nm} \times 65.5 = 78\ \text{nm}$ for the refractive index compensated results and together with the length drifts this hides the real changes of the refractive index on short measuring distances.

To cope with the instabilities of the interferometer head a much longer measuring range is helpful. The refractive index compensation relies on the length difference due to the dispersion for both wavelengths. A longer path leads to a larger difference. The uncertainty of this difference is dominated by a length independent part and therefore the relative uncertainty of this difference decreases with length. However, the overall uncertainty cannot be better than the basic stability of the set-up.

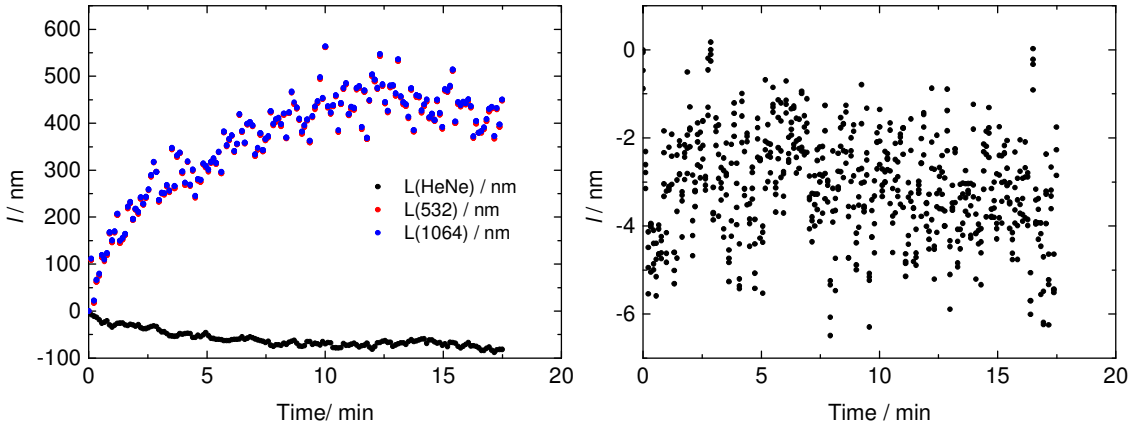

Figure 4: Midterm stability of the interferometer. Left figure: length results for 532 nm and 1064 nm and the HeNe reference. Right figure: difference between 532 nm and 1064 nm results.

Therefore the interferometer head was set up at the 50 m comparator of the PTB (geodetic base) in a folded beam path configuration with a HeNe reference interferometer. Due to the mechanical set-up the dead path was approximately 4 m. Since the comparator is not isolated from the floor, vibrations with 200 nm amplitude and 130 Hz frequency are present, depending on activities in the building and the surrounding area (in the night the vibrations are considerably smaller). On the positive side the vibrations allow a demonstration of the averaging process for the refractive index compensation in order to reduce the scaling effect for the uncertainty of the *A*-factor for the wavelengths used.

The vibrations are shown in the left part of figure 5 measured with the 532 nm wavelength at the position “0” of the comparator, corresponding to a measurement path of approx. 4 m for the interferometer.

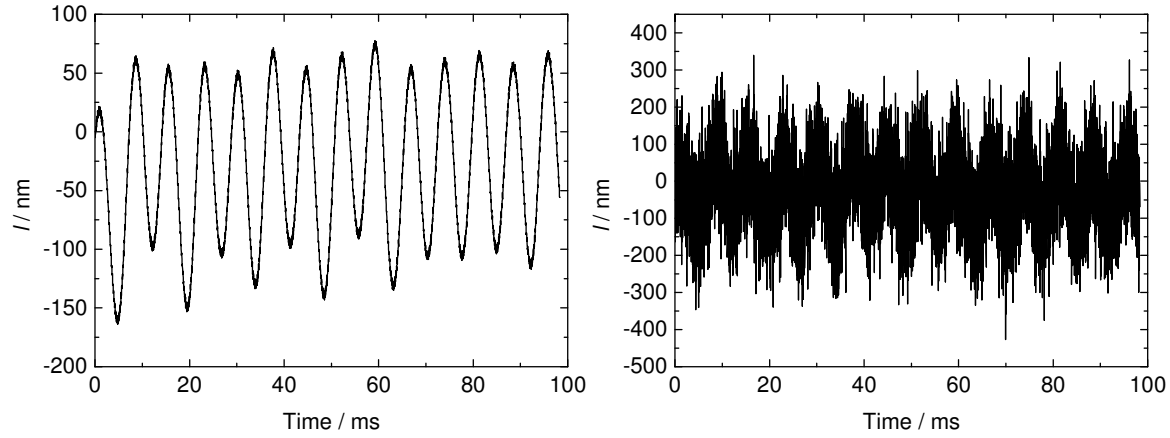

Figure 5: Length change with time at the zero position (4 m offset) for the 532 nm wavelength (left) and the refractive index compensated result without averaging (right).

When applying equation 6 for the refractive index compensation, the *A*-factor and the instability of the interferometer head significantly increase the uncertainty. The application of equation 6 on the measurements with both wavelengths leads to the result shown in the right part of figure 5. The vibrations are still visible but superimposed with a significant noise. Averaging the length results would reduce the noise but is not applicable for dynamic measurements and would not allow reproducing the vibrations correctly.
However, as a side effect of the compensation method, the effective temperature in the beam path can also be calculated from both length results, if the air pressure is known in addition to the partial pressure of water vapor. Since the temperature variations on time scales of the order of 10 ms are probably negligible, a moving average of the temperature can be calculated and used in combination with the measured air pressure and humidity to calculate an Edlen based refractive index for each data point.
According to equation 7 it seems easy to calculate the temperature, but the dead path of the interferometer has to be taken into account. If the interferometer counters are set to zero at an arbitrary position, the calculated temperature from the small length changes due to noise leads to arbitrary temperature values. When moving the reflector the dispersion comes into effect and stabilizes the temperature values. Simulations show that the direct compensation according to equation 6 is independent of the dead path but the calculated temperature depends on this. In the left part of figure 6 the calculated temperature for a measurement of 2 m length with the dead path of 4 m is shown together with the measured temperature. For this diagram 8192 samples corresponding to 98.3 ms were averaged. The positions 0 mm and 40 mm are not shown in the left part because they result into values around -273 °C. The calculated temperature starts with around 9 °C and settles to the measured value of approximately 21.2 °C. If a measured temperature for the dead path is used to add *nl* with the dead path of 4 m for both wavelengths before evaluating the temperature the calculated temperature data are much more reliable (figure 6, right part). It should be stated that this procedure is only necessary for the averaging process described next and only when the measurement starts with an arbitrary offset and is not an absolute distance measurement. The deviations between measured and calculated temperature are in the range ±0.15 K. A detailed uncertainty budget for the temperature is not yet available but there is a rule of thumb derived

from the Edlen equation, since a temperature change of 1 K changes the refractive index by 10^{-6}. In the opposite direction a measurement uncertainty for both lengths of 10^{-6} leads to an uncertainty of the calculated temperature of 1 K. This means that the ±0.15 K deviation leads to a length dependent measurement uncertainty part of the prototype of the order $1.5 \cdot 10^{-7}$.

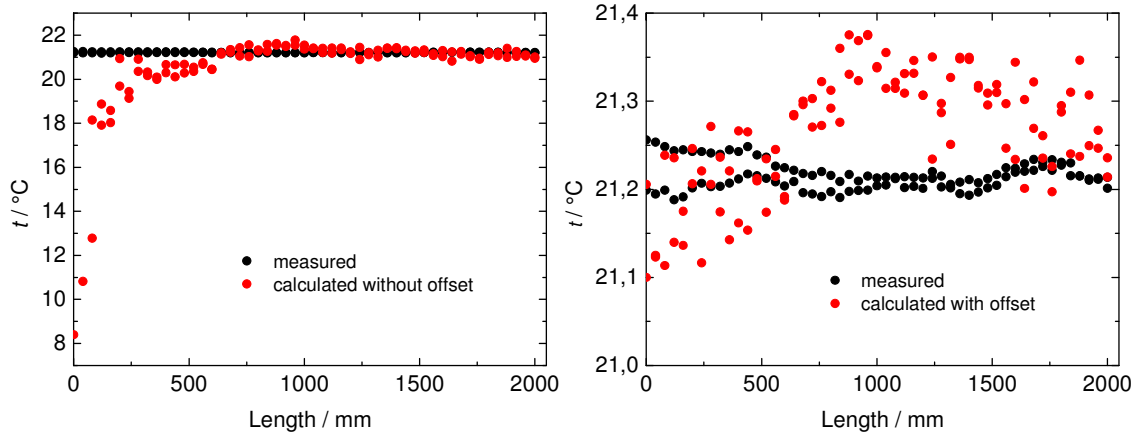

Figure 6: Calculated temperature from the dispersion without applying the dead path (left) and with dead path (right).

Now a single measurement at fixed position "0" is considered. Calculating the temperature with a 4 m offset with the measured temperature the result for an 8192 data block corresponding to 98.3 ms is shown in the left part of figure 7. There is no visible temperature change and the standard deviation is 0.022 K. With a moving average of 1024 temperature values (12.3 ms) a variation of only 11 mK during the 98 ms is derived (right part of figure 7). Knowing the instability of the interferometer head it cannot be decided if this temperature change is real or an artifact of the instability.

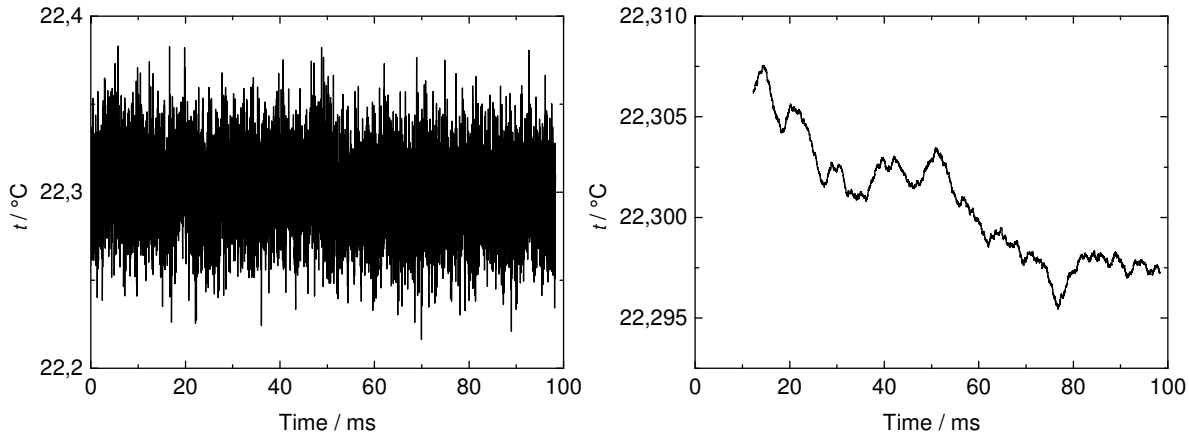

Figure 7: Calculated temperature from raw phase values without averaging (left) and with 1024 sample averaging (12.3 ms, right).

Using the averaged temperatures together with the measured humidity and the air pressure the refractive index compensated result can be calculated. Figure 8 shows the difference between the standard Edlen based result (left part of figure 5) and the refractive index compensated result without (left) and with temperature averaging (right). The standard deviation without averaging is 90 nm, with averaging the changes of the temperature are reflected. In the stable part between 80 ms and 96 ms the standard deviation is 3.5 nm. The standard deviation is

therefore reduced by a factor of 25 compared to a theoretical value of $\sqrt{1024} = 32$. As stated before, it cannot be identified if the changes are really due to the refractive index or the stability of the interferometer.

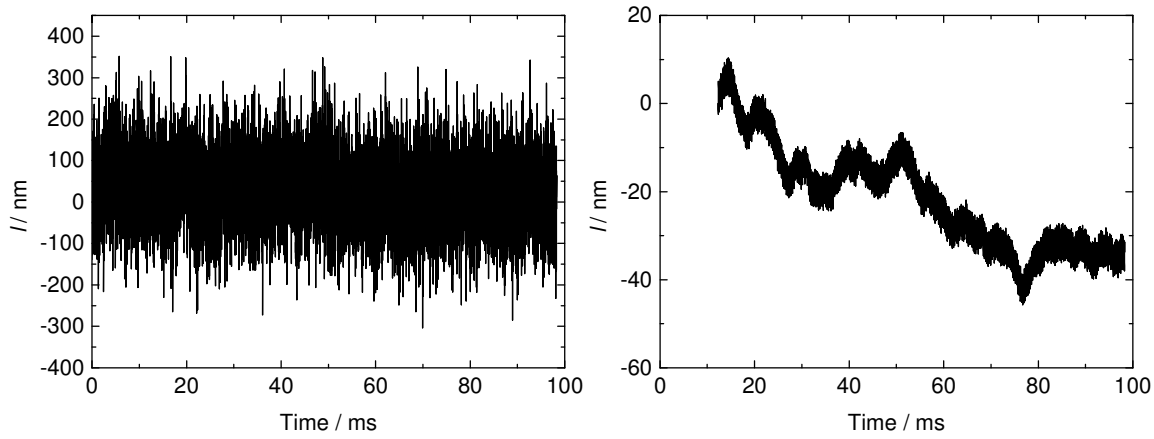

Figure 8: Difference between refractive index compensated and Edlen based result. Left: without averaging. Right: with 1024 sample averaging.

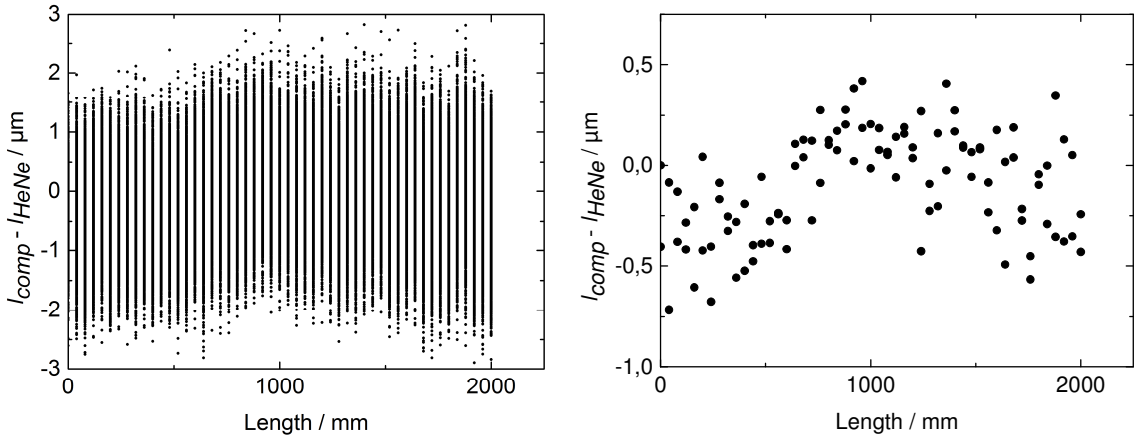

Figure 9: Difference between both refractive index compensated results and the HeNe reference interferometer. Left: without averaging, right: with.

The difference between the refractive index compensated interferometer and the HeNe reference of a measurement from zero to a length of 2 m and back to zero in 40 mm steps is shown in figure 9. Without temperature averaging the scatter is up to ±3 µm, with averaging within -0.7 µm and +0.4 µm. In both cases the scatter is not length dependent and resembles the mechanical stability of the prototype interferometer head. The achievable uncertainty without these instabilities can be estimated from the evaluated temperature and is of the order $1.5 \cdot 10^{-7}\ l$ for the observed deviations of ±0.15 K.

5. CONCLUSION AND OUTLOOK

The prototype of a refractive index compensated tracking interferometer was developed and tested without the tracking capability. Despite the poor mechanical stability of the standard optomechanical components used for the prototype two important results were obtained. The signal to noise ratio of a heterodyne interferometer utilizing a steel sphere as one reflector is

sufficient for refractive index compensation with its higher demand on the basic uncertainty due to the scaling factor of 65.5. The second important result is that via averaging over optically measured temperatures the influence of the scaling factor can be greatly reduced while retaining the time resolution of the position measurements. The averaged temperatures deviate within ±0.15 K from the conventionally measured ones which indicates that the targeted uncertainty of 10^{-7} *l* for the final interferometer seems achievable.

6. ACKNOWLEDGEMENT

This work was funded by the EMRP Project IND53. The EMRP is jointly funded by the EMRP participating countries within EURAMET and the European Union.

REFERENCES

[1] http://www.etalon-ag.com/
[2] K. B. Earnshaw and J. C. Owens, "Dual wavelength optical distance measuring instrument, which corrects for air density", IEEE J. Quantum Electron. **3**, 544-550 (1967)
[3] K. Meiners-Hagen and A. Abou-Zeid, “Refractive index determination in length measurement by two-colour interferometry”, Meas. Sci. Technol. **19**, 084004 (5pp) (2008)
[4] B. Edlén, "The refractive index of air", Metrologia **2**, 71-80 (1966)
[5] G. Bönsch, E. Potulski, "Measurement of the refractive index of air and comparison with modified Edlen’s formula", Metrologia **35**, 133-139 (1998)
[6] P. Köchert, J. Flügge, C. Weichert, R. Köning, and E. Manske, “A fast phasemeter for interferometeric applications with an accuracy in the picometer regime”, 10th IMEKO Symp. Laser Metrology for Precision Measurement and Inspection in Industry vol 2156 (Düsseldorf: VDI) 251–8 (2011).

CONTACTS

Dr. K. Meiners-Hagen Karl.Meiners-Hagen@ptb.de
Dr. Denis Dontsov Dontsov@sios.de